Solution- and Bound-State Conformational Study of *N*,*N*′,*N*″-Triacetyl Chitotriose and Other Analogous Potential Inhibitors of Hevamine: Application of trNOESY and STD NMR Spectroscopy

Antje Germer,[a] Clemens Mügge,[b] Martin G. Peter,[a] Antje Rottmann,[a, c] and Erich Kleinpeter*[a]

Abstract: The solution-state conformations of *N*,*N*′,*N*″-triacetyl chitotriose (**1**) and other potential chitinase inhibitors **2**–**4** were studied using a combination of NMR spectroscopy (NOESY) and molecular mechanics calculations. Determination solely of the global energy minimum conformation was found to be insufficient for an agreement with the NMR results. An appropriate consistency between the NMR experimental data and theoretical calculations was only reached by assessing the structures as population-weighted average conformers based on Boltzmann distributions derived from the calculated relative energies. Analogies, but also particular differences, between the synthetic compounds **2**–**4** and the naturally-occurring *N*,*N*′,*N*″-triacetyl chitotriose were found. Furthermore, the conformation of compounds **1** and **2** when bound to hevamine was also studied using transferred NOESY experiments and the binding process was found to impart a level of conformational restriction on the ligands. The preferred conformation as determined for **1** in the bound state to hevamine belonged to one of the conformational families found for the compound when free in solution, although full characterisation of the bound-state conformations was impeded due to severe signal overlap. Saturation transfer difference NMR experiments were also employed to analyse the binding epitopes of the bound compounds. We thus determined that it is mainly the acetyl amido groups of the trisaccharide and the heterocyclic moiety which are in close contact with hevamine.

Keywords: carbohydrates · chitotriose · conformation analysis · molecular modelling · NMR spectroscopy

Introduction

Chitinases are enzymes capable of cleaving the bond between two consecutive *N*-acetyl glucosamine residues of chitin, a major component of the cell wall of many fungi and the exoskeleton of insects and crustaceans. Chitinases have been found in a wide range of organisms including bacteria, which degrade chitin as a source of carbon,[1, 2] as well as crustaceans and insects, for which the enzymes perform an essential function during growth and moulting,[3] and fungi or even plants. The function of chitinases in plants seems to be to provide the plant with a general means of defence against attack by fungal pathogens and insects.[4] Therefore, these proteins and their inhibitors are of general interest to many fields of study. One well known chitinase is hevamine,[5] an enzyme which can be isolated from latex freshly tapped from the rubber tree *Hevea brasiliensis*. Based on the amino acid sequence and protein folding, hevamine belongs to the family of 18 chitinases.[6] The structure of hevamine is well characterised; the crystal structure has been refined to an *R* value of 1.8 and the reaction mechanism for hydrolysis is understood quite well, at least theoretically.[7–10] In addition to further clarification of the reaction mechanism, the binding characteristics of various hevamine ligands are also important for the design of new transition state analogues which may act as chitinase inhibitors and therefore represent potential insecticides[11, 12] and/or fungicides.[13]

In order to design novel potential inhibitors rationally, a fundamental understanding of the underlying molecular mechanism of the interaction of hevamine with carbohydrate substrates is essential. Thus, it is important to verify whether or not the bound conformation of natural saccharides is also

[a] Prof. Dr. E. Kleinpeter, A. Germer, Prof. Dr. M. G. Peter, Dr. A. Rottmann
Institut für Organische Chemie und Strukturanalytik
Universität Potsdam, Am Neuen Palais 10
14415 Potsdam (Germany)
Fax: (+49)-331-977-5064
E-mail: kp@chem.uni-potsdam.de

[b] Dr. C. Mügge
Institut für Chemie, Humboldt Universität Berlin
Brook-Taylor-Strasse 2, 12489 Berlin (Germany)

[c] Dr. A. Rottmann
Scienion AG
Volmerstrasse 7b, 12489 Berlin (Germany)

DOI: 10.1002/chem.200204231

maintained by synthetic analogues. In the last few years, new NMR-based screening methods, for example the transferred nuclear overhauser enhancement spectroscopy (trNOESY), have been developed to characterise the binding process; this NMR experiment allows access to the stereochemistry of the ligand in the bound state.[14–16] A further technique, the recently reported saturation transfer difference (STD) NMR method, allows determination of binding epitopes.[17, 18] The observation of binding-induced changes in the chemical shift or the flexibility (relaxation measurements) of the protein residues or the ligand itself provide further insight.[19]

Herein, the conformation and binding of oligosaccharide inhibitors **2**–**4** and the substrate analogues of *N*,*N*′,*N*″-triacetyl chitotriose (**1**) to hevamine have been studied (see Figure 1). A complete array of 1D and 2D NMR spectroscopic techniques was employed for the structural characterisation and spectral assignment of the ligands **1**–**4**. A study of

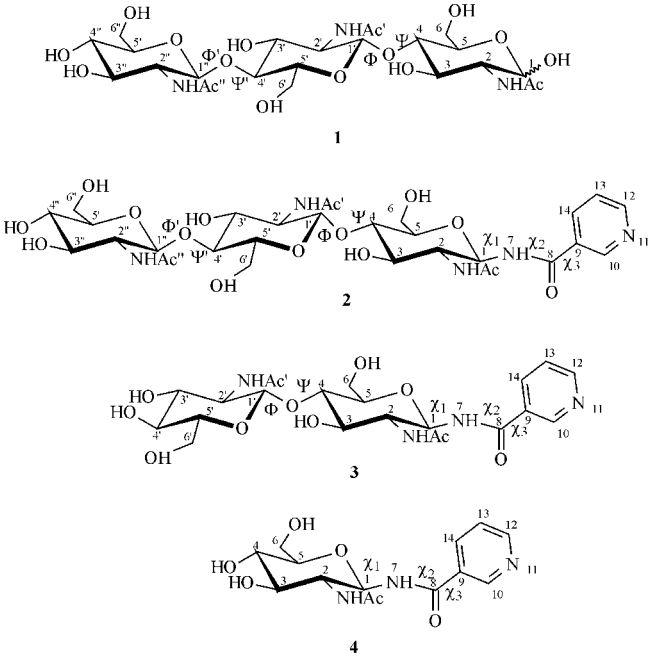

Figure 1. The structures of *N*,*N*′,*N*″-triacetyl chitotriose (**1**) and the synthetic potential inhibitors **2**–**4**. The bonds about which the torsional angles Φ, Ψ, Φ', Ψ', χ_1, χ_2 and χ_3 occur are indicated. The numbering scheme employed is also indicated.

both the solution-state conformations and the hevamine-bound conformation of the compounds **1**–**4** was also performed. For the conformational analysis of the hevamine-bound conformations, and the determination of binding itself, trNOESY experiments were utilised. To unequivocally define the binding epitopes of the carbohydrate ligands, STD NMR experiments on the hevamine-bound compounds were performed. The STD experiments have only recently been introduced as a tool for screening compound mixtures for binding activity and for determining binding epitopes.[17, 18] The NMR experiments were furthermore complemented by modelling studies utilising molecular mechanics calculations. The results obtained for compound **3**[20, 21] were then compared with the conformational behaviour of **2** and **4** as described in the following.

Results and Discussion

Molecular mechanics calculations: Since the measured NOE values represent population-weighted averages of all participating conformers, the NMR data alone, therefore, can rarely define the population of oligosaccharides unambiguously. Therefore the conformational analysis of these compounds requires additional molecular modelling methods to complement the experimental NMR data. Thus, population-weighted average conformations were calculated for the complete number of accessible conformations for compounds **1**–**4** and then compared with the experimentally observed NOE data. Each molecule was subjected to an extensive conformational search and grid search simulations were run to calculate relaxed potential energy maps for Φ and Ψ.

For the molecular modelling, we used a distance depending dielectric constant of 78 to implicitly consider the presence of the solvent water. To take thus solvent effect into account, is particularly important in the modeling of carbohydrates due to their extremly strong tendency to form inter/intramolecular hydrogen bonds. We were aware of the difficulty of this approach in case of solvents which could be also be involved in hydrogen bonding. However, since the charge screening is the most important solvent influence, this approach should provide good results. Larwood et al.[22] who among others studied the solvation effects on the conformational behaviour of gellan with explicit and implicit inclusion of water found out that there are no differences in the location of the minimum energy conformations around the glycosidic linkage, although there were differences in the orientation of some of the hydroxyl groups, and as expected, the hydroxyl groups of such residues were involved in hydrogen bonding with water molecules.[23]

In order to further justify our approach, we studied the solvation energy during the MD simulation in the presence of water molecules exemplary for compound **3**: six minima conformations around the glycosidic linkage of **3** were subjected to the MD simulation in a box of explicit water molecules, as described in more detail in ref. [20]. The minimum energy conformations were restricted to aggregates, that is their relative geometry is not be optimized. Therefore, only the interaction energy of compound **3** and water was calculated. These calculations proved very similar solvation energies to be present in all minimum energy conformations ($\Delta E_{solv} \approx \pm 1$ kcal mol^{-1}). From these results, it was concluded, that it is sufficient to consider the solvent in an implicit manner only along the calculation of the present disaccharide fragment, as long as the differences in the orientation of the hydroxyl groups in the two different models are considered correctly.

Concerning the conformational search of the hydroxymethyl group, only the *gt* and the *gg* orientations of the exocyclic portion were explicitly taken into account. Thus, four combinations for each disaccharidic unit in **1**–**3** were taken into account, namely *gg-gg*, *gg-gt*, *gt-gg* and *gt-gt*; accordingly, these four initial conformations were considered. As reported previously, we found out that the shape of the potential energy surface is independent of the initial conformation of the hydroxymethyl group.[24] Population-weighted averages were

then calculated from the local minima conformations thus obtained by using Boltzmann distributions[25] calculated from the relative energies of the conformers. The internuclear distances in a system with N possible non-degenerate states can be calculated by:

$$d = \sum_{i=1}^{N} f_i d_i \quad (1)$$

where f_i is a normalised weighting factor for state i, given by:

$$f_i = \frac{q_i}{\sum_{i=1}^{N} q_i} \quad (2)$$

The quantity q_i is the individual partition function of state i, which is defined as:

$$q_i = -\frac{\Delta E}{RT} \quad (3)$$

where ΔE is the energy difference between state i and the ground state, R the gas constant, and T the absolute temperature.

Conformation of the glycosidic bond: The adiabatic surface calculated with respect to the torsional angles Φ and Ψ for compound **1** using the AMBER 4.1 force field routine which is implemented in the SYBYL program[26] is presented in Figure 2.

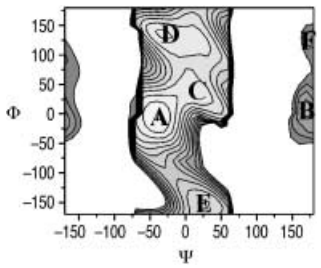

Figure 2. Conformational map with respect to the torsional angles Φ and Ψ for compound **1**. Population densities are indicated by contour lines; position A represents the global minimum, B – F other local minima.

Six different conformational families (A – F) were found for the glycosidic linkage C1′-O-C4. The same conformational families were obtained for the same glycosidic linkage in the other potential inhibitors **2** and **3**. This result is in slight contrast to the report of Aida et al.[23] who found chitobiose as a highly populated single conformer of the linkage domain; but it concurs with the results of Espinosa et al.[24] who indicated the existence of more than one populated region. In both studies, a global minimum in the region of A was obtained which is the expected conformation for the β-(1 → 4) glycosidic linkage.[27–29] However, it is generally accepted that the generated minima conformations strongly depend on the force field used and in comparison to Espinosa who predicted the global minima at Φ +54° and Ψ 0° using the AMBER force field parameterised by Homans[30] for carbohydrates, the global minimum in this work was calculated to be at Φ −8° and Ψ −39° using the AMBER force field parameterised by Woods[31] for carbohydrates. Nevertheless, there is still another local minimum conformation at Φ +36° and Ψ +7° near that global minimum. Furthermore, the dominance of the global minimum (Espinosa 84 %) is somewhat reduced in our calculations on compound **3** (A, 70 %). The most striking difference between the calculated minima conformations about the C1′-O-C4 glycosidic bond lies in the number of local minima conformations, in this work six local minima conformations (A – F) were calculated compared to three by Espinosa et al.[24] However, only the A (70 %) and B (25 %) conformations were found to be densely populated; for C – F, only about 1 % contribution for each conformer was found.

For compounds **1** and **2**, each of the low energy conformations, A – F, with respect to the glycosidic bond C1′-O1-C4, was set as the starting point for the next run of grid search simulations for finding minima about the torsional angles Φ' and Ψ' of the second glycosidic bond C1″-O1-C4′. Similar local minima conformations A – F were also found for the C1″-O1′-C4′ linkage, resulting in a total of 36 local conformational minima overall. Of these 36 conformational minima for **1**, nine were populated by more than 1 % (see Table 1). Similar results with respect to the conformations of the glycosidic linkage were obtained for **2** and therefore these local conformational minima about the glycosidic linkages evidently do not depend on the presence or absence of an aglycon at C1. The four most populated conformations of **1** are depicted in Figure 3.

Table 1. Torsion angles Φ, Ψ, Φ', and Ψ' for the predicted local conformational minima of **1** with a population in excess of 1 %.

Conformer	C1′-O-C4 Dihedral angles		C1″-O-C4′ Dihedral angles		Population [%]
	Φ	Ψ	Φ'	Ψ'	
1	−8	−40	13	174	34
2	13	174	13	174	26
3	−8	−40	−8	−40	16
4	13	174	−9	−40	11
5	−9	−40	146	2	1
6	36	6	13	174	1
7	−8	−40	40	8	1
8	13	174	36	4	1
9	36	4	−8	−40	1

Regarding the torsional angles χ_1, χ_2 and χ_3 of the conformational minima for compounds **2** – **4**, χ_1 has two local minima at about 0° and about 180°; a *trans* conformation is highly favoured for χ_2 and the high flexibility about χ_3 shows two local minima at 0 and 180° in each case for each of the three compounds **2** – **4**. All these minima have been verified for compounds **2** – **4** using ab initio quantum-mechanical calculations.

The calculated, and moreover expected, elongated orientation of the heterocyclic moiety for compounds **2** – **4** with respect to the pyranose rings was consistent with the NMR data (see below) in so far as interresidual NOEs between the middle *N*-acetyl glucosamine residue and the heterocyclic ring were not detected.

NMR studies: The full assignment of the ^{1}H and ^{13}C NMR signals of each compound was accomplished using the whole

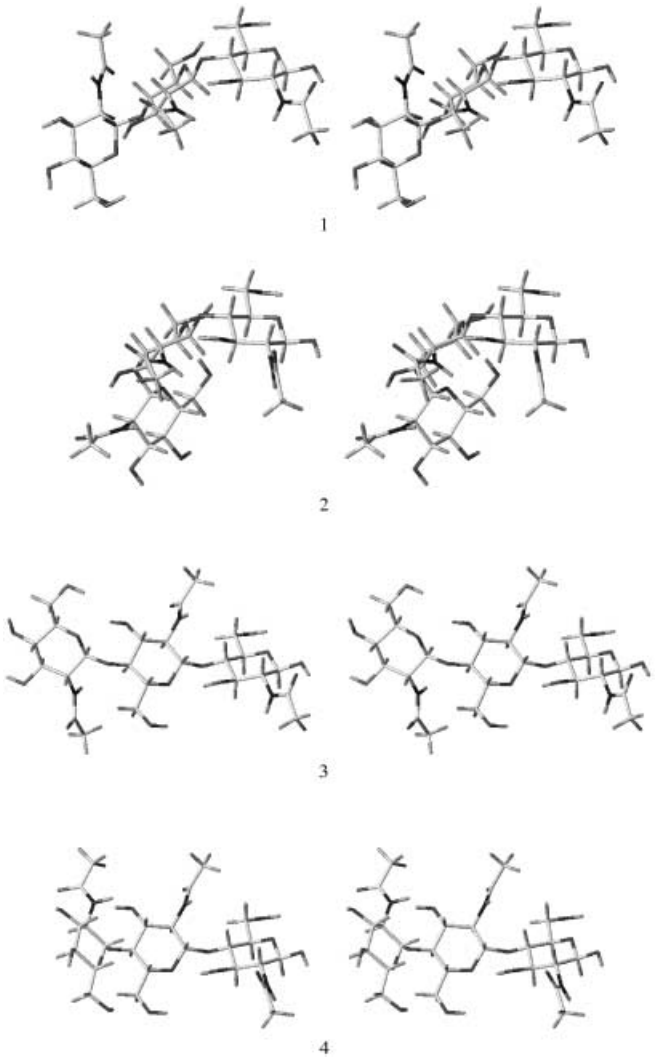

Figure 3. Four of the most populated, low energy conformers of **1** (1, 34%; 2, 26%; 3, 16%; 4, 11%).

arsenal of 1D and 2D NMR techniques. The spectrally distinct anomeric protons were useful entry points into the spin systems and the application of DQF-COSY, TOCSY and HMQC experiments, corroborated by the additional application of HMQC-TOCSY experiments, provided the assignments of each sugar residue. HMBC spectra were acquired for both the assignment of the quaternary carbons and to substantiate the interresidue linkages. The distinction between the α- and β-anomers of **1** was facilitated by the fact that the anomeric proton in the α-anomer, in comparison to the β-anomer, was significantly more downfield and $^3J_{H1,H2}$ was considerably smaller, $\approx$2.5 Hz, due to the relative disposition of H1 and H2 (cf. the *trans* diaxial orientation of H1 and H2 in the β-anomer). Although the analysis was routine in method, it was not necessarily straightforward due to severe signal overlap and the use of 3D HMQC-TOCSY was found to be necessary to alleviate this problem. As an example, Figure 4 shows the COSY spectrum of **1**. The ^{1}H and ^{13}C chemical shifts for compounds **1**–**4** are presented in Tables 2 and Table 3, respectively.

The validity of the theoretical results for the adopted conformations was examined using NMR and was based essentially on NOESY measurements. Compounds **1**–**4** were subjected to 2D NOESY experiments utilising mixing times of 200, 400, 600 and 1000 ms.

However, because of the severe signal overlap and because of the uncertainty in the dynamic properties of different parts of the compounds, namely the carbohydrate and heterocyclic residues, strict quantitative analysis was not possible. Only the upper and lower bounds of interproton distances could be estimated by calibration against known distances such as the distance between H1 and H3 (2.64 ± 0.01 Å) of the non-reducing residue of *N*-acetyl glucosamine (GlcNAc). Nevertheless, the intensities of all the NOE cross peaks at different mixing times were determined using spectrometer routines, compared to the intensities of the NOE cross peak between H1 and H3 and assessed as very strong ($d_{H,H} < 2.8$ Å), strong (2.8 Å $< d <$ 3.2 Å), medium (3.2 Å $< d <$ 3.6 Å) and weak (3.6 Å $< d <$ 4 Å).

As an example, NOEs involving the anomeric protons are displayed in Figure 5 for compound **1** (see below).

The interresidue NOEs of significance for compounds **1**–**3** are presented in Table 4 together with the population-weighted internuclear distances of all conformational minima.

The data in Table 4 clearly indicate that it is not possible to simultaneously justify all of the observed NOEs by the one conformer. For example, at least qualitatively, the presence of the NOEs between H1′ and H3α/β and between H1″ and H3′ for **1** indicate that the conformational minimum B is heavily populated. Furthermore, the NOE between H1′ and H4α and between H1″ and H4′ also indicates the presence of conformer A and/or C. This is confirmed by NOEs between H1′ and the two H6-pro*S* and between H1″ and the two H6-pro*S*′, which are indicative for the minima C and D. Thus a NOE could only be observed if the orientation of the hydroxymethyl group occupies a *gt* orientation (the population-weighted average of the internuclear distance between H1″ and the two H6-proS′ is ca. 3.54 Å for **1**). Finally, no indicative NOE could be detected for minima E and F, but the absence of an NOE does not necessarily mean that these conformers are completely absent.

From a quantitative point of view, the population-weighted distances obtained from the molecular mechanics distribution were compared with the NOE values obtained experimentally. It can be observed that the agreement is satisfactory, and that the conformational behaviour could be explained by a dynamic equilibrium consisting of the six minima A–F. It should be noted that whilst the population of the local minima A and B dominate, the agreement between the theoretical and experimental results is much better if all conformations are taken into account and indeed also the rotation about the torsional angles χ_1, χ_2 and χ_3. Especially for compound **3**, the dominance of the minima A and B are expressed by a strong NOE between H1′ and H4 and between H1′ and H3. For compounds **1** and **2**, the changes in the strength of the NOEs compared with **3** is indicative of a change in the population of the minima about the glycosidic linkages and a change in the number of the higher-populated conformations. For compounds **2**–**4**, interresidual NOEs between the *N*-acetyl glucosamine units and the heterocyclic unit were not observed

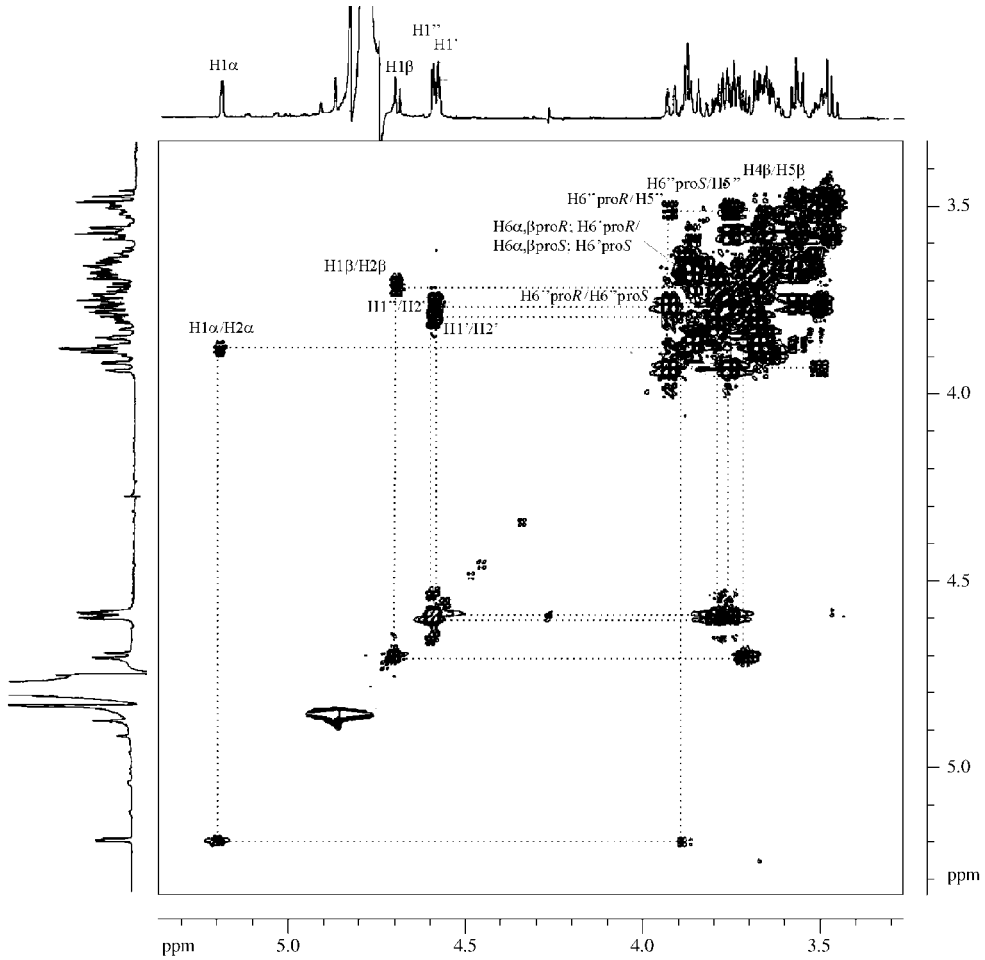

Figure 4. DQF-COSY spectrum of compound **1**.

Table 2. ^{1}H chemical shifts $\delta(^{1}H)$ [ppm] for compounds **1**–**4**.

Compound	Unit	H1, H10	H2, H12	H3, H13	H4, H14	H5	H6-pro*S*, H6-pro*R*	Me	$^{3}J_{H1,H2}$
1,*α*	GlcNAc	5.20	3.89	3.89	3.64	3.90	3.68, 3.80	2.05	2.56
anomer	GlcNAc′	4.59	3.78	3.73	3.65	3.57	3.69, 3.86	2.06	8.46
	GlcNAc″	4.60	3.76	3.58	3.48	3.50	3.76, 3.93	2.07	8.40
1,*β*	GlcNAc	4.71	3.71	3.70	3.62	3.52	3.68, 3.84	2.05	8.14
anomer	GlcNAc′	4.59	3.78	3.73	3.65	3.57	3.68, 3.86	2.06	8.46
	GlcNAc″	4.60	3.76	3.58	3.48	3.50	3.76, 3.93	2.07	8.40
	GlcNAc	5.20	3.89	3.88	3.63	3.64	3.66, 3.86	1.98	9.73
2	GlcNAc′	4.59	3.78	3.73	3.64	3.56	3.66, 3.86	2.07	8.09
	GlcNAc″	8.84	3.75	3.57	3.48	3.50	3.75, 3.93	2.07	8.27
	heterocycle	4.60	8.61	7.52	8.24	–	–	–	–
	GlcNAc	5.29	4.02	3.84	3.70	3.69	3.70, 3.87	1.98	9.63
3	GlcNAc′	4.63	3.76	3.58	3.48	3.50	3.76, 3.92	2.08	8.38
	heterocycle	8.86	8.72	7.59	8.15	–	–	–	–
4	GlcNAc	5.20	3.89	3.60	3.48	3.52	3.69, 3.82	1.88	9.65
	heterocycle	8.75	8.61	7.49	8.06	–	–	–	–

consistent with an elongated, linear orientation of the rings as predicted by the modelling results.

In summary, the minima about the glycosidic linkage are dominated by the *exo*-anomeric conformations about *Φ* (minima A–C) as proposed similarly by Espinosa et al.[24] and by Aida et al.[23] for this part of **1**–**3**.The crystal structure analysis[32] of chitobiose also revealed the same conformation about *Φ*. The predominant *syn-Φ,Ψ* conformer (minima A and C) could be corroborated for chitobiosyl derivative **3**. However, for chitotriosyl derivatives **1** and **2**, the dominance of the *syn-Φ,Ψ* conformer is reduced at the gain of the *syn-Φ*/*anti-Ψ* conformer. Conclusively, the *syn-Φ,Ψ*–*syn-Φ′*/*anti-Ψ′* and *syn-Φ*/*anti-Ψ*–*syn-Φ′*/*anti-Ψ′* conformers are most populated in the chitotriosyl derivatives **1** and **2**.

Table 3. ^{13}C NMR chemical shifts $\delta(^{13}C)$ [ppm] for compounds **1**–**4**.

Compound	Unit	C1, C8	C2, C9	C3, C10	C4, C12	C5, C13	C6, C14	acetyl Me, carbonyl
1, ***α***	GlcNAc	90.3	53.5	69.0	79.4	69.8	59.9	21.9, 173.7
anomer	GlcNAc′	101.1	54.8	72.0	78.9	74.3	60.5	21.8, 173.8
	GlcNAc″	101.3	55.4	73.2	69.5	75.7	59.8	21.8, 173.9
1, ***β***	GlcNAc	94.6	55.9	72.3	78.9	74.4	59.8	21.9, 173.7
anomer	GlcNAc′	101.1	54.8	72.0	78.9	74.3	59.9	21.8, 173.8
	GlcNAc″	101.3	55.4	73.2	69.5	75.7	60.5	21.8, 173.9
	GlcNAc	95.0	57.8	68.8	83.3	83.3	64.2	26.5, 178.2
2	GlcNAc′	105.7	59.0	76.2	83.4	78.8	64.2	26.5, 178.2
	GlcNAc″	105.9	59.2	77.7	73.9	80.2	64.8	26.6, 178.8
	heterocycle	173.4	140.6	153.4	155.0	128.5	142.0	
	GlcNAc	83.7	58.5	77.1	83.3	80.9	64.4	26.4, 179.4
3	GlcNAc′	105.9	60.1	77.9	74.2	80.4	65.1	26.6, 179.2
	heterocycle	173.6	133.3	152.2	156.7	128.8	140.9	–
4	GlcNAc	81.9	57.2	77.2	83.4	80.4	63.6	26.4, 179.3
	heterocycle	172.3	132.7	152.4	157.1	128.8	140.8	–

Binding studies to hevamine: Compounds **1**–**4** were subjected to comparative NOESY experiments in the presence and absence of hevamine. In the absence of hevamine, positive NOEs were observed for **1**–**4**, as is expected for small molecules. Upon the addition of hevamine, both compounds **1** and **2** displayed trNOEs as indicated by a reversal of the sign of the cross peaks (see Figure 5). Furthermore, these cross peaks showed a different sign to the diagonal peaks in trROESY experiments, thus excluding the possibility of protein-relayed or spin diffusion-mediated correlations. Hence, it can be concluded that both compounds **1** and **2** bind to hevamine within a range of 10^{-3}–10^{-7} M for K_D, which characterises the observation window for trNOESY. The trNOEs for compounds **1** and **2** are presented in Table 5. Unfortunately, full assignments were precluded in some instances due to extensive signal overlap.

Close scrutiny of the NOESY spectra recorded in the absence and presence of hevamine showed important and clear differences. Some of the cross peaks in the NOESY spectrum of the free ligand differ in their intensity in the trNOESY spectrum of the complex. In particular, for compound **1**, both the trNOEs between H1″ and H4′ and between H1′ and H4α/H4β were strong in comparison to the medium or weak NOEs observed in the free state, evidence that when bound to hevamine **1** is in the *syn*-Φ,Ψ-*syn*-Φ',Ψ' conformation (minima A and C). The medium to strong NOEs between H1″ and H6-pro*R*′ and between H1′ and H6-proR support a high population of the *syn*-Φ,Ψ conformation at both glycosidic linkages. Both observed NOE values, though, are best explained by the conformational minimum C (cf. Table 4). Minimum A can only explain a strong NOE between H1′ and H4 and minimum D can only explain a strong NOE between H1′ and H6-pro*R*. Population of both minima is unlikely however, and would, with a 50:50 distribution of A and D conformers, actually result in the observation of medium intensity NOEs instead of the observed strong ones. The NOE between H1′ and H3α/H3β was absent in the trNOESY spectrum. The position of a possible H1″/H3′ correlation is potentially overlapped by a possible H1′/H3′ correlation and ambiguity therefore arises. On the other hand, support for a medium size for the NOE by theoretical calculations (see Table 4) suggests that the cross peak should be assigned to a correlation between H1′ and H3′. These

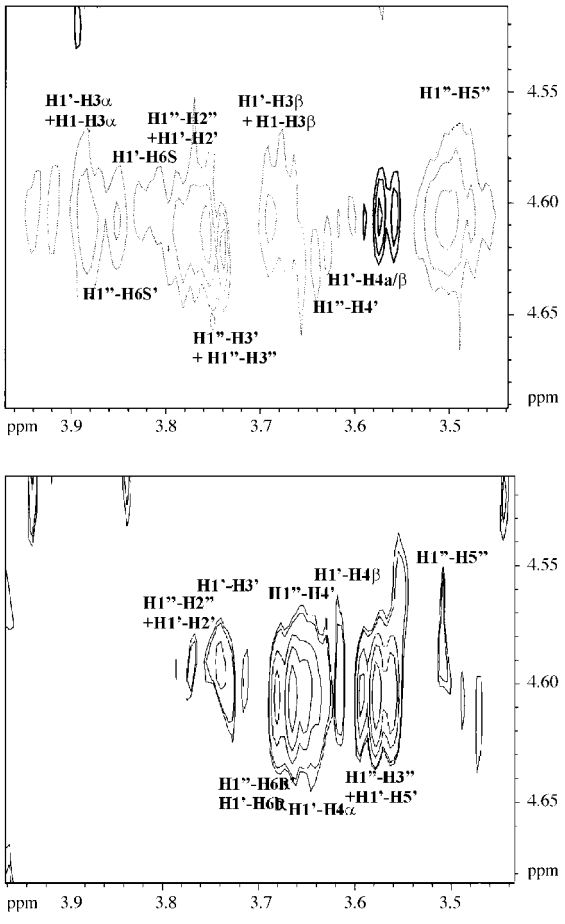

Figure 5. Comparison of 2D NOESY spectrum of **1** (top) with 2D trNOESY spectrum of **1** complexed to hevamine (bottom). Solid contour lines indicate negative cross peaks whilst broken contour lines describe positive cross peaks. Assignments are so indicated.

Table 4. Comparison of the intensity of interresidual NOEs from experimental NOESY spectra and the internuclear distances for all low-energy conformations of **1**–**3** obtained by force field calculations together with the population-weighted average values.

Compound	Hydrogens	Internuclear distances from modelling calculations for each conformer						Observed signal intensity[a]	Average internuclear distance[b]/ Å
		A	B	C	D	E	F		
	H1″, H4′	2.3	3.6	2.3	3.4	3.6	4.0	m-w	3.12
	H1″, H3′	3.6	2.2	4.5	4.5	4.3	3.2	s	2.71
	H1″, H6*S*′	4.1	3.4	2.5	2.9	3.7	3.7	m	3.54
1	H1′, H3α	3.6	2.2	4.5	4.5	4.3	3.2	m	3.03
	H1′, H4α	2.3	3.6	2.3	3.4	3.6	4.0	m-w	2.82
	H1′, H3β	3.6	2.2	4.5	4.5	4.3	3.2	m	3.03
	H1′, H6*S*	4.1	3.4	2.5	2.9	3.7	3.7	w	3.70
	H1″, H4′ (+ H5, H4)	2.3	3.6	2.3	3.4	3.6	4.0	vs	3.22
	H1″, H3′	3.6	2.2	4.5	4.5	4.3	3.2	s	2.71
2	H1″, H6′*S*	4.1	3.4	2.5	2.9	3.7	3.7	m	3.56
	H1′, H4 (+ H5, H4′)	2.4	3.6	2.3	3.4	3.6	4.0	vs	2.82
	H1′, H3	3.6	2.2	4.5	4.5	4.3	3.2	m	3.15
	H1′, H6*S*	4.1	3.4	2.5	2.9	3.7	3.7	m	3.75
	H1′, H4	2.3	3.6	2.3	3.4	3.6	4.0	vs	2.82
	H1′, H3	3.6	2.2	4.5	4.5	4.3	3.2	s	3.11
	H1′, H5	4.5	2.2	4.0	4.5	4.5	3.8	n.d.	3.65
3	H1′, H6*R*	4.4	4.5	2.9	4.3	4.7	5.4	n.d.	4.47
	H2′, H4	3.9	4.5	4.5	3.5	2.1	4.1	n.d.	4.17
	H2′, H5	4.7	4.8	4.7	4.8	4.3	2.6	n.d.	4.75
	H2′, H6*S*	3.1	4.5	4.0	5.2	2.8	2.2	n.d.	3.66

[a] vs, very strong (< 2.8 Å); strong (2.8–3.2 Å); m, medium (3.2–3.6 Å); w, weak (3.6–4 Å); nd, not detected. [b] Determined for the calculated structures.

features clearly indicate that the conformation in the bound state is the local minimum C of the *syn*-Φ,Ψ-*syn*-Φ',Ψ' family of **1**.

In the X-ray crystal structure determination of the *N*,*N*′,*N*″-triacetylchitotriose/hevamine complex (**1**),[33] the non-reducing residue was found to occupy subsite A. Molecular mechanics calculations revealed strong contacts between the acetamido methyl group of the non-reducing sugar with the Gly48 and Gly11 residues, the acetamido methyl group of the middle sugar showed strong interaction with Gly9 and the acetamido methyl group of the reducing sugar showed strong contacts with Trp255 along with contacts between (OH)-6″ and Gly69 and Ile82. The conformation about the glycosidic linkages were calculated as *syn*-Φ,Ψ (+17 and −34°, respectively) and *syn*-Φ',Ψ' (+32 and −6°, respectively). The overlay between the low energy conformer in the free state (global minimum A) and the bound conformer is depicted in Figure 6.

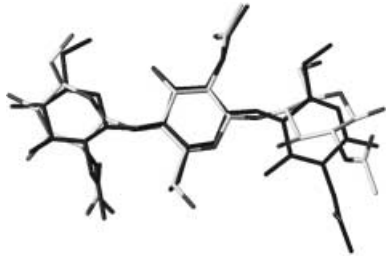

Figure 6. Superposition of the low energy solution-state conformation A of **1** and the calculated hevamine-bound conformation (dark-grey).

Considering the difference in energy between the conformation adopted in the bound state and the global minimum conformer for **1**, $\Delta E_{\text{deform.}} \approx 4$ kcal mol^{-1}, it is requisite that the binding energy should be at least of this magnitude. It is known that for the binding of a flexible compound to a protein, usually one of the conformations of the ensemble existing in the free state is preferred,[34, 35] but not exclusively as conformers, higher in energy, can also be present in the bound state.[36] In the former case, a negative binding entropy results leading to a decrease in the free energy of binding.

For compound **2**, changes in the NOE pattern in the absence and in the presence of hevamine were also discerned. In particular, the NOE between H1″ and H3′ disappears, evidence that the *syn*-Φ'/*anti*-Ψ' conformer (minima B) is not energetically favoured when **2** is complexed to hevamine. Unfortunately, the important glycosidic NOEs between H1″ and H4′ and between H1′ and H4 are overlapped with those of H5″ and therefore explicit information regarding the bound-state conformation was precluded. Since trNOEs could only be observed for **1** and **2**, that is compounds with at least three *N*-acetyl glucosamine residues, it is tempting to conclude that binding is strongest to the sugar units and is independent of the presence or absence of a heterocyclic moiety.

STD NMR experiments: The 1D saturation transfer difference (STD) NMR experiments were performed on all four compounds, **1**–**4**, in the presence of hevamine (ca. 100-fold excess of the ligands). As a difference spectrum, only signals from bound ligands are present thus permitting their immediate identification. This technique has the great advantage that it can be combined with any NMR pulse sequence and in the 1D mode, the method is fast and robust.[17] The results confirmed the binding indicated previously by trNOESY, that is compounds **1** and **2** bind to hevamine but compounds **3** and **4** do not; additionally though, the binding epitopes of the bound ligands were now able to be conclusively identified. For

example, the 1D STD NMR spectrum for compound **1** is presented in Figure 7. The significantly better results that are obtainable by the incorporation of a spinlock[17] (see bleow) are also highlighted in Figure 7.

An expansion of the aromatic and aliphatic region for compound **2** is depicted in Figure 8.

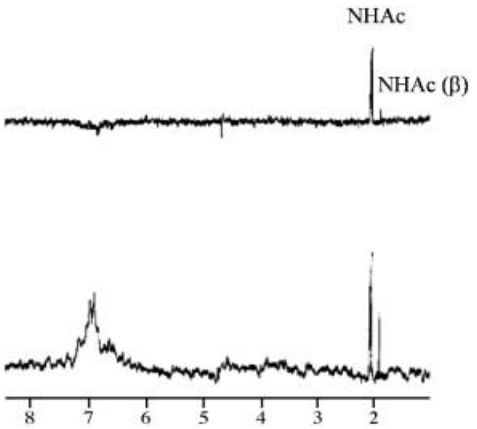

Figure 7. 1D STD NMR spectrum with spinlock (top) in comparison to an STD NMR spectrum without spinlock (bottom) for compound **1**.

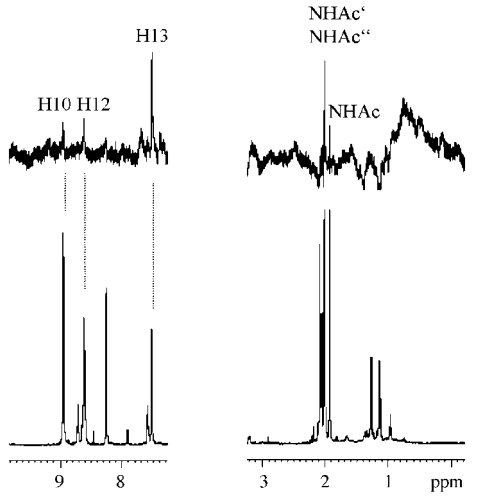

Figure 8. 1D STD NMR spectrum (top traces) in comparison to a normal proton NMR spectrum (bottom traces) in the presence of hevamine for compound **2** (the molar ratio of hevamine to compound **2** was approximately 1:100).

Prominent signals in the 1D STD NMR spectrum were the methyl protons of the N-acetyl groups in compound **1** and **2**. The saturation transfer was also efficient for the aromatic protons of compound **2** and indicate that these protons must be close to the protein surface. Some adjustment of the saturation time provided an indication that the methyl groups were closer to the protein surface than the aromatic protons. Despite saturation times of about 3 s, in the case of compound **1**, STD signals for the ring protons (which are also of smaller S/N ratio than the N-acetyl groups) could not be detected. To better resolve the spectral region of the ring protons, STD TOCSY NMR spectra were also acquired but additional information was not forthcoming (data not shown). Therefore, we suppose small dissociation rates for the studied system, which result in a smaller signal intensity in general.

To summarise, the STD NMR spectra confirm the results of the trNOESY spectra that both compounds **1** and **2** have binding activity to hevamine. The N-acetyl groups of the sugar residues are important for binding and should be closer to the protein surface than the other protons. These epitopes are depicted in Figure 9. Thus, despite the implication that the heterocyclic moiety does not appear to play a determinant role in the binding process, it is nevertheless in intimate contact with the protein.

Conclusion

Our studies furnished a comprehensive representation of the conformation of *N*,*N*′,*N*″-triacetyl chitotriose (**1**) and the potential inhibitors **2**–**4** in the free state, as well as of **1** and **2** when bound to hevamine. Utilising 2D NOESY experiments together with accompanying AMBER force field calculations, it was shown that the compounds adopt more than one conformation when free in solution as consensus between the NMR experimental data and the theoretical calculations was only reached by assessing the structures as population-weighted average conformers based on Boltzmann distributions derived from the calculated relative energies. Although quantitative analysis was restricted because of severe signal overlap, our experimental results were nevertheless confirmed by molecular mechanics calculations. trNOESY experiments indicated binding for compounds **1** and **2** but not for compounds **3** and **4** and it is therefore concluded that in order to bind to hevamine, at least three sugar residues are required for this series of compounds. Although the major requirement is that three sugars are present and that binding is independent of the presence of a heterocyclic moiety, nonetheless, the heterocyclic moiety is in intimate contact with the protein as established from STD experiments where it was clear that the closest binding epitopes of **1** and **2** consist of the N-acetyl groups of the sugar residues and for **2**, the aromatic heterocycle. The bound, and therefore bioactive

Table 5. Comparison of NMR data (intensity of interresidual trNOEs) and calculated values for the conformation of **1** and **2** in the ligand/hevamine complex obtained by force field calculations.

Compound	Hydrogens	Observed signal intensity[a]	Average internuclear distance[b]/ Å
1	H1″/H1′, H3′	m	4.3
	H1″, H4′	s	2.16
	H1′, H6-pro*R*	m-s	3.1
	or		
	H1″, H6-pro*R*′	m-s	3.9
	H1′, H4α	m-s	2.28
	H1′, H4β	m	2.28
2	H1″/H1′, H3′	s	4.4/2.54
	H1″, H6-pro*S*′	m	3.05
	H1′, H4/H4′	s	2.3/3.9
	or		
	H1″, H4′/H5″	s	2.2/2.4

[a] s, strong; m, medium. [b] Determined for the calculated structures. The experimental error in signal intensity was estimated to be less than 20%.

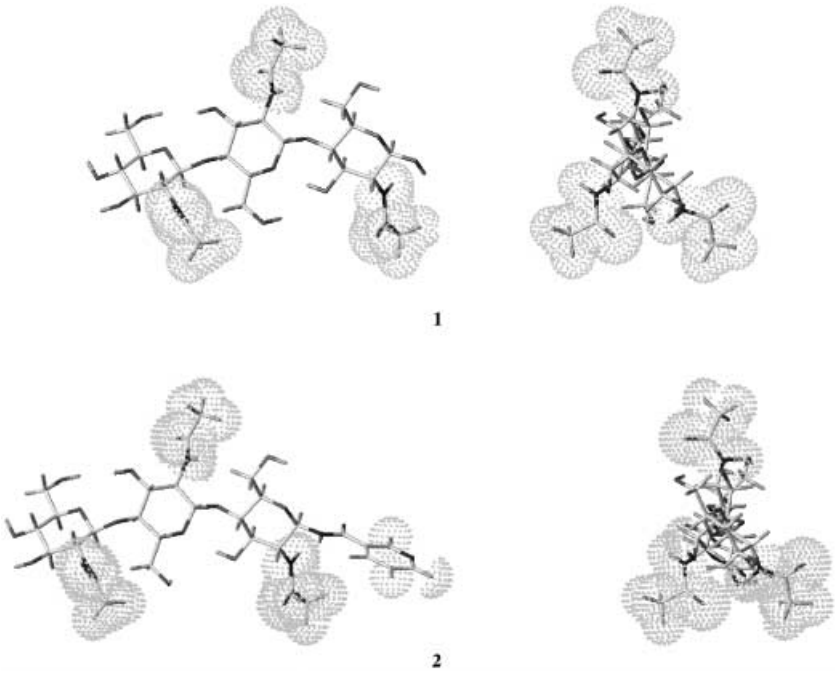

Figure 9. Orthographic view of the major binding epitopes of **1** (the bound conformation resulting from trNOESY studies is shown) and **2** (the supposed bound conformation from trNOESY studies) for binding to hevamine. The protons that were found to be in close contact with the protein surface are covered by a MOLCAD surface.

conformations, of **1** and **2** was near to the minimum conformation C (Table 4) of the glycosidic linkages of the two *N*-acetyl glucosamines. Thus, the combination of molecular mechanics calculations and NMR results together allowed a description of the conformational behaviour of compounds **1**–**3** with respect to the glycosidic linkage between two adjacent *N*-acetyl glucosamines and between the *N*-acetyl glucosamine unit and the heterocyclic unit in compounds **2**–**4**.

Experimental Section

Samples: Hevamine was isolated from freshly collected latex of *Hevea brasilienis* in the Laboratory of Biochemistry (J. J. Beintema), Rijksuniversiteit Groningen (The Netherlands). *N*,*N*′,*N*″-Triacetyl chitotriose (**1**) was isolated by standard procedures from a hydrolysate of chitin (cf.[37]). Compounds **3** and **4** were synthesized as described previously.[38]

***N*-[2-Acetamido-4-*O*-(2-acetamido-4-*O*-{2-acetamido-2-deoxy-β-D-glucopyranosyl}-2-deoxy-β-D-glucopyranosyl]-2-deoxy-β-D-glucopyranosyl]-nicotinic amide (2)**: EEDQ was added (29 mg, 0.12 mmol) to a solution of nicotinic acid (25 mg, 0.2 mmol) in dry CH_2Cl_2 (5 mL). After stirring for 12 h at RT, a solution of undecaacetylchitotriosyl amine[39] (50 mg, 0.054 mmol) in CH_2Cl_2 (2 mL) was added dropwise and stirring was continued for 120 h. The solvent was evaporated in vacuo. Et_2O was added and stirring was continued for 1 h. After filtration, the solid residue was analyzed by TLC and MS before the crude undecaacetylchitotriosylglycosl nicotinic amide was subjected to O-deacetylation. $R_f = 0.25$ ($CHCl_3$/acetone 1:3). MALDI-MS: *m*/*z*: 1064.4 $[M+K]^+$, 1048.5 $[M+Na]^+$, 1026.5 $[M+H]^+$.

Ammonia was passed through an ice-cold stirred solution of the crude undecaacetylchitotriosylglycosl nicotinic amide (55.4 mg, 0.054 mmol) in dry methanol (5 mL). The reaction vessel was sealed and stirring was continued at RT for another 24 h. The mixture was filtered over a Celite pad, the solvent was evaporated, and the solid residue was triturated under vigorous stirring with CH_2Cl_2 (5 mL) for 30 min. Chromatography on silica (MeOH) yielded **2** as colourless crystals (25 mg, 64 %). $R_f = 0.37$ (MeOH); m.p. 234–243 °C (decomp); $[\alpha]_D^{22} = +15.6$ ($c = 0.5$, H_2O); MALDI-MS: *m*/*z*: 770.3 $[M+K]^+$, 754.1 $[M+Na]^+$, 732.1 $[M+H]^+$; MALDI-HR-MS: *m*/*z*: calcd for $C_{30}H_{45}NaN_5O_{16}$: 754.2759; found: 754.2746 $[M+Na]^+$.

NMR Experiments: 600 MHz spectra were performed on a BRUKER AMX 600 NMR spectrometer at the Humboldt university of Berlin (group C. Mügge). Solutions of 1–5 mg of samples **1**–**4** and of hevamine, respectively, were lyophilised twice from 1 mL of D_20 (99.8 % deuteriated) prior to dissolution in 700 μL of D_2O. All NMR experiments were carried out in oxygen-depleted solutions which were obtained by purging the NMR samples in situ with argon for 30 min. In the binding experiments, the molar ratio of hevamine to ligand was 1:30 for the trNOESY and 1:100 for the STD NMR experiments. Spectra were recorded at 313 and 298 K without sample spinning using the HDO signal as an internal reference (4.78 ppm at 313 K). Data acquisition and processing were performed with XWIN-NMR software (Bruker). For assignment of the ^1H and ^{13}C NMR spectra, DQF-COSY, phase-sensitive HMQC, HMBC, and HMQC-TOCSY spectra were measured. NOESY, ROESY and TOCSY spectra were all recorded in phase-sensitive mode. The relaxation delay was set at 2 s in each case and the mixing times were chosen as 200, 400, 600 and 1000 ms for the NOESY experiments. To suppress Hartmann-Hahn magnetisation transfer, 2D ROESY experiments were performed with a mixing time of 250 ms and a spin-locking field of 2–3 kHz. For the 2D TOCSY experiments, the mixing time was set to 80 ms and the spin-locking field was 8 kHz. For all 2D NMR spectra, a total of 2k (F_2) × 512 (F_1) data points were recorded. Sixty-four transients were accumulated for each F_1 data point. The residual HDO signal was suppressed by presaturation when necessary.

2D trNOESY Experiments on **1**–**4** were recorded with a total of 2 k (F_2) × 512 (F_1) data points for each experiment. The HDO signal was suppressed by low-power presaturation during the relaxation and mixing times. The total relaxation delay was 1.2 s. Mixing times of 150, 300 and 600 ms were utilised. The interproton distances were obtained from volume integrals employing H1 and H3 as a reference spin pair and a distance approximation of 2.64 Å between the protons.

For 1D STD experiments,[17] saturation transfer was achieved by using 39 selective 1 k Gaussian 90° pulses with a duration of 50 ms and a spacing of 1 ms. For one set of spectra, the protein envelope was irradiated at 1.2 ppm (on-resonance) and 20 ppm (off-resonance). Another set of spectra was generated by setting the on-resonance frequency to 7.2 ppm. Saturation times were 0.5, 1.0, 1.5 and 2 s. The relaxation delay was set to 4 s for compound **1** and 12 s for compounds **2**–**4**. STD TOCSY spectra were recorded with 256 increments with 32 transients per increment using a MLEC 17 spin-lock field of 60 ms at 7.5 kHz. The relaxation delay was set at 4 s for compound **1** and 12 s for compound **2**.

Molecular mechanics calculations: Molecular mechanics calculations were run either on a Silicon Graphics O2 R5000 or a Silicon Graphics Origin 24 × R10000 workstation. All calculations were run with the AMBER 4.1 force field implemented in the SYBYL 6.4[24] program. Based on GLYCAM 93[31] parameters, a new set of parameters was developed for compounds **2**–**4** that is consistent with AMBER (details to be published elsewhere). Dihedral angles at the glycosidic and other interresidual linkages are defined as follows (cf. Figure 1):

Φ = H1′-C1′-O-C4 and Ψ = C1′-O1′-C4-H4 for compounds **1**–**3**;

Φ' = H1″-C1″-O-C4′ and Ψ' = C1″-O-C4′-H4′ for compounds **1** and **2**;

χ_1 = H1-C1-N7-C8, χ_2 = C1-N7-C8-C9, and χ_3 = N7-C8-C9-C10 for compounds **2**–**4**.

Glycosidic bond angles at the beginning of the calculations were fixed at 117° and the pyranose rings were treated as rigid units adopting a $^4C_1$ conformation. The dihedral angle ω (O5-C5-C6-O6) was not explicitly restrained. Only the *gt* and *gg* conformation was taken into account for the lateral chain of the GlcNAc moieties.[40, 41] The N-acetyl group was fixed in an energetically lower *trans* position. Furthermore, the assumption that every state is equally degenerate was made; a distance dependent dielectric constant of 78.0 was used; interactions for all compounds **1**–**4** were scaled by a factor of 0.83; and a cut-off for the nonbonding interactions at 12 Å was also applied. Thus, in first step the relaxed potential energy maps were calculated for the corresponding glycosidic linkage Φ,Ψ using a grid step of 10° for compounds **1**–**3** and for χ_1 and χ_3 for compound **4**. χ_2 was found to be in the energetically lower *trans* position. Every point of this map was optimised using 1000 gradient iterations. From these relaxed maps, adiabatic surfaces were built and the probability distributions calculated for each Φ,Ψ point according to the Boltzmann function at 313 K. In the last step, each of the local minima point Φ,Ψ was used as a starting point for Φ' and Ψ' for **1** and **2** and χ_1 and χ_3 for **3**, resulting in 6 additional potential energy maps. The resulting combinations of local minima $\Phi,\Psi-\Phi',\Psi'$, $\Phi,\Psi-\Phi',\Psi'-\chi_1,\chi_3$ and $\Phi,\Psi-\chi_1\chi_3$ were then re-optimised.

Bound-state molecular modelling: Protein co-ordinates were taken from the crystal structure described by Terwisscha van Scheltinga et al.[33] Glycosidic torsion angles for compounds **1**–**4** were set to those described in the free state. The starting orientations for the sugar residues were chosen to match the relative position of **1** in the crystal structure and were obtained by fitting the new compound over **1** and afterwards deleting **1**.

Atomic charges were AMBER charges. For the complex, all energy calculations were carried out using the AMBER 4.1 force field. A cut-off of nonbonding interaction at 20 Å was applied. Energy minimisations were then conducted on the different complexes using a gradient termination of 0.05 kcal mol^{-1} Å.

Acknowledgement

This work was supported by EU grant no. BIO4-CT-960670. Financial support from the Studienstiftung des Deutschen Volkes is gratefully acknowledged (scholarship to A. G.). M.G.P. acknowledges partial support by the Fonds der Chemischen Industrie.

[1] K. J. Kramer, L. Corpuz, H. K. Choi, S. Muthukrishnan, *Insect Biochem. Mol. Biol.* **1993**, *23*, 691–701.
[2] A. S. Sahai, M. S. Manocha, *FEMS Microbiol. Rev.* **1993**, *11*, 317–338.
[3] D. P. Morgavi, M. Sakurada, Y. Tomita, R. Onodera, *Microbiology* **1994**, *140*, 631–636.
[4] D. B. Collinge, K. M. Kragh, J. D. Mikkelsen, K. K. Nielsen, U. Rasmussen, K. Vad, *Plant J.* **1993**, *3*, 31–40.
[5] B. L. Archer, *Phytochemistry* **1976**, *15*, 297–300.
[6] B. Henrissat, *Biochem. J.* **1991**, *280*, 309–316.
[7] A. C. Terwisscha van Scheltinga, S. Armand, K. H. Kalk, A. Isogai, B. Henrissat, B. W. Dijkstra, *Biochemistry* **1995**, *34*, 15619–15623.
[8] A. C. Terwisscha van Scheltinga, M. Henning, B. W. Dijkstra, *J. Mol. Biol.* **1996**, *262*, 243–257.
[9] K. A. Brameld, W. D. Shrader, B. Imperiali, W. A. Goddard III, *J. Mol. Biol.* **1998**, *280*, 913–923.
[10] K. A. Brameld, W. A. Goddard III, *J. Am. Chem. Soc.* **1998**, *120*, 3571–3580.
[11] S. Sakuda, A. Isogai, S. Matsumo, A. Suzuki, *Tetrahedron Lett.* **1986**, *27*, 2475–2478.
[12] D. Koga, A. Isogai, S. Sakuda, S. Matsumo, A. Suzuki, S. Kimura, A. Ide, *Agric. Biol. Chem.* **1987**, *51*, 471–476.
[13] A. Schlumbaum, F. Mauch, U. Vögeli, T. Boller, *Nature* **1986**, *324*, 365–367.
[14] T. Peters, B. M. Pinto, *Curr. Opin. Struct. Biol.* **1996**, *6*, 710–720.
[15] L. Y. Lian, I. L. Barsukov, M. J. Sutcliffe, K. H. Sze, G. C. K. Roberts, *Methods Enzymol.* **1994**, *239*, 657–700.
[16] B. Meyer, T. Weimar, T. Peters, *Eur. J. Biochem.* **1997**, *246*, 705–709.
[17] M. Mayer, B. Meyer, *Angew. Chem.* **1999**, *111*, 1902–1906; *Angew. Chem. Int. Ed.* **1999**, *38*, 1784–1788.
[18] M. Mayer; B. Meyer, *J. Am. Chem. Soc.* **2001**, *123*, 6108–6117.
[19] A. Poveda, J. Jiménez-Barbero, *Chem. Soc. Rev.* **1998**, *27*, 133–144, and references therein.
[20] A. Germer, M. G. Peter, E. Kleinpeter, *J. Org. Chem.* **2002**, *67*, 6328–6338.
[21] A. Germer, S. Klod, M. G. Peter, E. Kleinpeter, *J. Mol. Model.* **2002**, *8*, 231–236.
[22] V. L. Larwood, B. J. Howlin, G. A. Webb, *J. Mol. Model.* **1996**, *2*, 175–186.
[23] M. Aida, Y. Sugawara, S. Oikawa, K. Umemoto, *Int. J. Biol. Macromol.* **1995**, *17*, 227–235.
[24] J.-F. Espinosa, J. L. Asensio, M. Bruix, J. Jiménez-Barbero, *J. An. Quim. Int. Ed.* **1996**, *92*, 320–324.
[25] P. W. Atkins in *Physikalische Chemie*, VCH, Weinheim, **1988**.
[26] SYBYL 6.4, Molecular Modelling Software, Tripos, Inc., St. Louis, Missouri, USA, **1997**. The AMBER force field used in this work had been parameterised for sugars. See also ref. [36] for an account of this method.
[27] B. R. Leeflang, J. F. G. Vliegenhardt, L. M. J. Kroon-Batenburg, B. P. van Eijck, J. Kroon, *Carbohydr. Res.* **1992**, *230*, 41–62.
[28] M. K. Dowd, A. D. French, P. J. Reilly, *Carbohydr. Res.* **1992**, *233*, 15–27.
[29] S. B. Engelsen, S. Perez, I. Braccini, C. Herve du Penhot, *J. Comput. Chem.* **1995**, *16*, 1096–1119.
[30] S. Homans, *Biochemistry* **1990**, *29*, 9110–9118.
[31] R. J. Woods, R. A. Dwek, C. J. Edge, B. Fraser-Reid, *J. Phys. Chem.* **1995**, *99*, 3832–3846.
[32] F. Mo, *Acta Chem. Scand.* **1979**, *A33*, 207–214.
[33] A. C. Terwisscha van Scheltinga, K. H. Kalk, J. J. Beintema, B. W. Dijkstra, *Structure* **1994**, *2*, 1181–1189.
[34] M. Gilleron, H.-C. Siebert, H. Kaltner, C. W. van der Lieth, T. Kozar, K. M. Halkes, E. Y. Korchagina, N. V. Bovin, H. J. Gabius, J. F. G. Vliegenthart, *Eur. J. Biochem.* **1998**, *252*, 416–427.
[35] J. L. Asensio, J. F. Espinosa, H. J. Dietrich, F. J. Cañada, R. R. Schmidt, M. Martín-Lomas, S. André, H. J. Gabius, J. Jiménez-Barbero, *J. Am. Chem. Soc.* **1999**, *121*, 8995–9000.
[36] A. García-Herrero, E. Montero, J. L. Muñoz, J. F. Espinosa, A. Vián, J. L. García, J. L. Asensio, F. J. Cañada, J. Jiménez-Barbero, *J. Am. Chem. Soc.* **2002**, *124*, 4804–4810.
[37] O. Scheel, J. Thiem, in *Chitin Handbook* (Eds.: R. A. A. Muzzarelli, M. G. Peter), Atec, Grottammare, **1997**, pp. 165–170; D. Schanzenbach, C.-M. Matern, M. G. Peter, in *Chitin Handbook* (Eds.: R. A. A. Muzzarelli, M. G. Peter), Atec, Grottammare, **1997**, pp. 171–174.
[38] A. Rottmann, B. Synstad, V. G. H. Eijsink, M. G. Peter, *Eur. J. Org. Chem.* **1999**, 2293–2297.
[39] J. P. Ley, M. G. Peter, *J. Carbohydr. Chem.* **1996**, *15*, 51–64.
[40] K. Bock, J. Duus, *J. Carbohydr. Chem.* **1994**, *13*, 513–543.
[41] Y. Nishida, H. Hori, H. Ohrui, H. Meguro, *J. Carbohydr. Chem.* **1988**, *7*, 239–250.

Received: July 5, 2002
Revised: January 3, 2003 [F4231]

